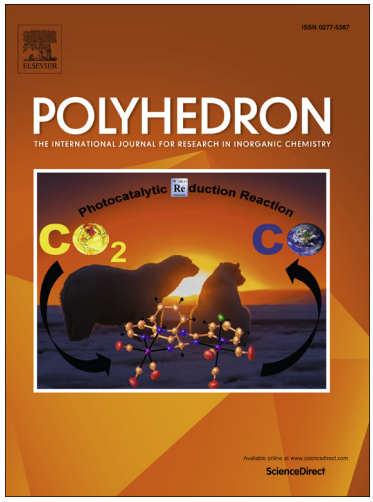

Synthesis and spectroscopic characterization of a new tripodal hexadentate iron chelator incorporating catechol units

Carla Queirós, Andreia Leite, Ana M.G. Silva, Paula Gameiro, Baltazar de Castro, Maria Range

PII: S0277-5387(14)00661-5
DOI: http://dx.doi.org/10.1016/j.poly.2014.10.003
Reference: POLY 11012

To appear in: *Polyhedron*

Received Date: 26 July 2014
Accepted Date: 7 October 2014

Please cite this article as: C. Queirós, A. Leite, A.M.G. Silva, P. Gameiro, B. de Castro, M. Range, Synthesis and spectroscopic characterization of a new tripodal hexadentate iron chelator incorporating catechol units, *Polyhedron* (2014), doi: http://dx.doi.org/10.1016/j.poly.2014.10.003

Synthesis and spectroscopic characterization of a new tripodal hexadentate iron chelator incorporating catechol units

Carla Queirós,[a] Andreia Leite,[a] Ana M. G. Silva,*[a] Paula Gameiro,[a] Baltazar de Castro,[a] Maria Rangel*[b]

[a] *REQUIMTE, Departamento de Química e Bioquímica, Faculdade de Ciências da Universidade, Rua do Campo Alegre s/n, 4169-007 Porto, Portugal*

[b] *REQUIMTE, Instituto de Ciências Biomédicas de Abel Salazar, Rua Jorge Viterbo Ferreira, nº 228, 4050-313 Porto, Portugal*

E-mail addresses: mcrangel@fc.up.pt, ana.silva@fc.up.pt

Abstract

We report the synthesis and physicochemical properties of a new tripodal hexadentate chelator (**catTHC**) synthesized by reaction of a flexible tripodal backbone with three bidentate catechol units. To improve the efficiency of the amide coupling reaction, classical conditions using two pairs of coupling reactants were tested, and a significant reduction in reaction time was achieved by using microwave irradiation with the reactants DCC/HOBt. Subsequent removal of the benzyl protecting groups using BCl_3 in dichloromethane provided the final chelator in good yield. The acid-base properties of **catTHC** in aqueous solution and the affinity of the ligand towards iron(III) were investigated at variable pH and in the presence of iron(III) using spectroscopic methods. The hexadentate ligand forms a 1:1 complex with iron(III) whose stability constant was determined by competition with EDTA. The values obtained for the stability constant and pFe^{3+} are log β_{110} = 36.70 and pFe^{3+} = 26.7.

Keywords: hexadentate chelators, iron(III) complexes, affinity constants, microwave-assisted coupling reaction

Introduction

The design of new biomimetic siderophores is a field of extensive and continuing research that aims to find ideal candidates for: (a) iron removal agents to be used in the treatment of iron overloaded patients [1,2,3]; (b) iron complexes as iron delivery agents in agriculture [4,5], and (c) iron removal in environmental applications [6,7]. Biomimetic siderophores are also applied in the study of iron metabolism and iron uptake in living systems [8] antibiotic drug-delivery strategies [9,10,11,12,13] and detection of iron(III) [14].

Siderophores are iron-specific chelators produced by microorganisms, fungi and plants which are used to scavenge iron from the environment and make this essential element available to the organisms. Siderophores can be divided in four broad groups based on the chemical nature of the chelating units: catechol, hydroxamate, hydroxypyridones and aminocarboxylic acids [15]. The characterization of catecholate siderophores was initiated in 1958 after the identification of a glycine conjugate of 2,3-dihydroxybenzoic acid when growing *Bacillus subtilis* under low-iron conditions [4]. Among natural siderophores containing catecholate ligands, enterobactin (Fig. 1) isolated from *Salmonella typhimurium* in 1970 is on the top of the affinity scale for iron(III), with log β_{110} (Fe^{3+})=49.0 and pFe^{3+}=35.5 [16].

Our group has been investigating the potential anti-microbial activity of a set of iron tripodal 3-hydroxy-4-pyridinone hexadentate chelators and the results revealed that the fluorescent ligands, in particular a rhodamine derived chelator, (CP777=4=MRB7), are effective in inhibiting the intramacrophagic growth of *Mycobacterium avium* [17,18,19]. All chelators are based on the same chelating unit and compound **CP256** (Fig. 1) was isolated to assess the chelating properties of the new compounds. The acidity and iron(III) stability constants were determined for **CP256**, which showed an affinity for iron (log β_{110} (Fe^{3+})=34.4 and pFe^{3+}=29.8) higher than those previously reported for mycobacterial siderophores (log β_{110}(Fe^{3+})=31 and pFe^{3+}=29.0) [18].

Since we aim to design antimicrobial agents based on the concept of their ability to restrict the iron sources in bacteria and taking into consideration the extremely high affinity of catecholate ligands for iron, we decided to synthesise a hexadentate catecholate ligand,

catTHC (Fig. 1), based on the same tripodal unit used for **CP256** and three catecholate bidentate units.

Since in **CP256** the tripodal backbone has terminal carboxylate functions, then an amide bond can be formed by reaction with a catecholamine. This will lead to structural differences between **CP256** and enterobactin; while in enterobactin the amide connector is directly linked to the catechol through -CONH- function, in **catTHC** the connector is inverted (-NHCO-) and there is an additional CH_2 spacer between the amide function and the catechol unit. Therefore, the electronic density of the catecholate ring is more affected by amide bond in enterobactin than in **catTHC**. Considering this structural differences, also differences in binding modes to iron are expecting to be achieved. While for the ferric enterobactin two binding modes are possible with different conformation stabilities and previous studies showed that the protonated salicylate binding mode is energetically favoured over the protonated catecholate mode,[20] for **catTHC**, we are expecting a lower stability constant with iron(III) than the one reported for enterobactin [16], although the catechol chelating unit should provide higher stability constants compared with 3,4-HPO ligands.

(Please insert Figure 1)

Material and methods

Reagents and solvents were purchased as reagent-grade and used without further purification unless otherwise stated. NMR spectra were recorded on a Bruker Avance III 400 spectrometer, operating at 400.15 MHz for protons and 100.62 MHz for carbons, equipped with pulse gradient units, capable of producing magnetic field pulsed gradients in the z-direction of 50.0 G/cm. Two-dimensional $^{1}H/^{1}H$ correlation spectra (COSY), gradient selected $^{1}H/^{13}C$ heteronuclear single quantum coherence (HSQC) and $^{1}H/^{13}C$ heteronuclear multiple bond coherence (HMBC) spectra were acquired using the standard Bruker software. Mass spectra were obtained from Unidade de Espectrometria de Masas of Santiago de Compostela and microanalyses were obtained from Unidad de Análisis Elemental of Santiago de Compostela. Flash chromatography was carried out using silica gel purchased from Merck (230-400 mesh). Electronic absorption spectra were recorded on

a Shimadzu – UV 3600 UV-Vis-NIR equipped with a Shimadzu TCC-Controller. A Crison pH meter Basic 20+, equipped with a combined glass electrode (model 50 29), and standardized at 25 ºC, was used for the spectrophotometric titrations.

Synthesis

*4-acetamido-4-(2-carboxyethyl)heptanedioic acid (**1**)*

Compound **1** [18] was synthesized through the reaction of nitromethane and *tert*-butyl acrylate, followed by reduction of the nitro to amino group with Raney nickel using the methodology described by Newkome and co-workers [21]. Further acylation with acetyl chloride and removal of the protecting *tert*-butyl groups using formic acid afforded anchor **1** [18].

*2,3-dibenzyloxybenzylamine (**2**)*

Compound **2** was prepared from benzylation of 2,3-dihydroxybenzaldehyde with benzyl bromide followed by condensation with *tert*-butylcarbamate in the presence of triethylsilane and subsequent hydrolysis in TFA using a reductive amination protocol [22].

*Protected hexadentate ligand (**3**)*

Compound **3** was synthesised using two different strategies involving: (a) the use of 1-[3-dimethylamino)propyl]-3-ethylcarbodiimide hydrochloride (EDAC)/*N*-hydroxysuccinimide (NHS) at room temperature and (b) the use of *N*,*N*'-dicyclohexylcarbodiimide (DCC)/N-hydroxybenzotriazole (HOBt) under microwave irradiation.

a) Using EDAC/NHS at room temperature: to a solution of 4-acetamido-4-(2-carboxy-ethyl)heptanedioic acid **1** (0.20 g, 0.70 mmol) in anhydrous DMF (4.0 mL) EDAC (0.48 g, 2.56 mmol) and NHS (0.30 g, 2.56 mmol) were added, under argon atmosphere and the reaction mixture was protected from light. After stirring for 4.5 h, EDAC (0.080 g, 0.40 mmol) was added and the reaction proceeded for two more hours, then 2,3-dibenzyloxybenzylamine **2** (0.84 g, 2.56 mmol) was added. The stirring was maintained for 64 h. Then the reaction mixture was purified by flash chromatography using a mixture of chloroform-methanol (9:1) as eluent giving compound **3** (0.70 g, 84 %);

b) Using DCC/HOBt under microwave irradiation: a mixture of 4-acetamido-4-(2-carboxyethyl) heptanedioic acid **1** (0.05 g, 0.18 mmol), DCC (0.13 g, 0.63 mmol) and HOBt (0.08 g, 0.59 mmol) in anhydrous DMF (0.6 mL) was placed in a 10 mL reaction vial, which was then closed under argon atmosphere and placed inside the cavity of a CEM microwave reactor. The reaction vial was irradiated at 55 ºC (1 min ramp to 55 ºC and 15 min hold at 55 ºC, using 100W maximum power). Then, the vessel was open to add 2,3-dibenzyloxybenzylamine **2** (0.20 g, 0.63 mmol) and anhydrous DMF (1.0 mL), re-closed under argon atmosphere and placed inside the cavity of a CEM microwave reactor. The reaction vial was irradiated at 55 ºC (1 min ramp to 55 ºC and 30 min hold at 55 ºC, using 100W maximum power). The purification protocol followed was the same used in the standard conditions (0.12 g, 56 %).

^{1}H NMR (DMSO-d$_6$, 400 MHz) δ: 1.77 (s, 3H, CH_3), 1.80-1.84 and 2.03-2.07 (2m, 12H, 6xCH_2), 4.23 (d, 6H, J= 5.7 Hz, 3x HNC$\underline{H}_2$), 4.97 and 5.17 (2s, 12H, 6xC$\underline{H}_2C_6H_5$), 6.82 (dd, 3H, J= 7.5 and J= 1.6 Hz, H-catechol), 7.02 (dd, 3H, J= 8.1 and J= 7.5 Hz, H-catechol), 7.07 (dd, 3H, J= 8.1 and J= 1.6 Hz, H-catechol), 7.18 (s, 1H, NH), 7.30-7.42 and 7.49-7.51 (2m, 30H, 6x $CH_2C_6\underline{H}_5$), 8.16 (t, 3H, J= 5.7 Hz, 3x $\underline{H}NCH_2$). ^{13}C NMR (DMSO-d$_6$, 100 MHz) δ: 23.5, 29.5, 30.0, 36.8, 56.5, 69.9, 73.9, 112.8, 120.3, 123.9, 127.6, 127.8, 128.18, 128.22, 128.4, 133.3, 137.0, 137.5, 145.1, 151.3, 168.8, 172.1, 174.5. MS (FAB) *m/z*: 1193 $[M+H]^+$.

*Deprotected hexadentate ligand (**catTHC**)*

To a solution of the protected hexadentate ligand **3** (0.35 g, 0.29 mmol) in anhydrous dichloromethane (5.0 mL), at 0 ºC, boron trichloride solution – 1M in CH_2Cl_2 (1.4 mL, 1.58 mmol) was added drop-by-drop, under argon atmosphere. The reaction mixture was allowed to warm to room temperature and the stirring was maintained for 16 h. Methanol (5.0 mL) was added and the reaction mixture was stirred for 1 h. The solvent was evaporated and the product was washed in acetone, evaporated and dried in high vacuum, giving ligand **catTHC** (0.13 g, 67%).

^{1}H NMR (DMSO-d$_6$, 400 MHz) δ: 1.77 (s, 3H, CH_3), 1.80-1.84 and 2.06-2.09 (2m, 12H, 6xCH_2), 4.09-4.17 (m, 6H, 3xHNC$\underline{H}_2$), 6.50-6.60 (m, 6H, H-catechol), 6.66 (dd, 3H, J= 6.8 and J= 2.4 Hz, H-catechol), 7.15-7.25 (m, 7H, NH and 6xOH), 8.34-8.40 (m, 3H,

HNCH$_2$). ^{13}C NMR (DMSO-d$_6$, 100 MHz) δ: 23.4, 29.5, 30.6, 37.8, 55.9, 114.1, 118.6, 125.9, 128.5, 142.9, 145.2, 168.8, 173.0. MS (FAB) *m/z*: 653 $[M+H]^+$. Anal. Calcd. for $C_{33}H_{40}N_4O_{10}.2H_2O.2CH_3COCH_3$: C, 56.92; H, 7.10; N, 6.81; Found: C, 56.94; H, 7.13; N, 6.53.

Spectrophotometric measurements

All solutions were prepared with double de-ionized water (conductivity less than 0.1 μS cm^{-1}). For the spectroscopic data, pH values of the different solutions were measured and UV-Vis spectra were record, at each pH. Spectra were recorded at (25.0±0.1 ºC) in 1 cm quartz cuvettes with a slit width of 2 nm in the range 225-800 nm. The global equilibrium constants were defined by Eqs. (1) and (2):

$$p[\mathrm{M}] + q[\mathrm{L}] + r[\mathrm{H}] \rightleftharpoons [\mathrm{M}p\mathrm{L}q\mathrm{H}r] \qquad (1)$$

$$\beta_{pqr} = \frac{[M_pL_qH_r]^{2p-q+r}}{[M]^p[L]^q[H]^r} \qquad (2)$$

where [M] represents the metal ion, [L] the hexadentate catecholate ligand (**catTHC**), $[H]^+$ the proton and p, q, r the stoichiometric coefficients of the metal ion, ligand and proton respectively. Distribution diagrams were plotted using the program Hyss 2006 [23] and the error associated to the log β_{pqr} value was determined using the Albert & Sergeant theory [24].

Determination of acidity constants

Spectrophotometric pH titrations were performed in stock solutions of both ligands ~5×10^{-5} M and ~6×10^{-5} M for the bidentate (2,3-dihydroxybenzaldehyde) and the hexadentate ligand (**catTHC**), respectively, in water (I = 0.1 M NaCl, 25 ºC) and aliquots of strong acid or base were added to adjust pH to the desired value. The pK_a values were calculated using the program pHab 2006 [25]. Calculations were performed with data from at least four independent measurements, considering the previous equations (1 and 2).

EDTA Competition Titrations

Solutions containing ~2.0×10^{-4} M hexadentate catecholate ligand (**catTHC**), ~2.0×10^{-4} M Fe(III) and ~1.2×10^{-3} M EDTA, in 0.1 M NaCl were used. Aliquots of strong acid or base solutions were added to 3 mL aliquots of the solution, containing **catTHC**, Fe(III) and EDTA, to adjust pH to the desired value (pH from 5 to 12) at 25 ºC. Solutions were allowed to achieve equilibrium for 24 h. The metal-complex stability constant was determined by competition studies with the hexadentate ligand EDTA by spectrophotometric methods and calculated using the program pHab 2006 [25]. The values of the stability constants are the average values of four independent experiments. The equilibrium constants of the hexadentate catecholate ligand, EDTA, Fe(III) formation constants for EDTA, the presence of the hydroxide species of iron and the autoprotolysis of water were taken into account [26].

Results and Discussion

*Synthesis of **catTHC***

In order to prepare a ligand with the most appropriate geometry for iron(III) binding, it is essential that the backbone is connected to the chelating units through the *ortho* positions relative to the oxygen coordinating atoms [27,28]. Therefore a methylamine group was introduced in the *ortho* position to the hydroxyl groups of the catechol unit. The advantage of having a methylamine in this position is that, by reacting with carboxylate groups provide the formation of an amide functionality which can form intramolecular hydrogen bonds, responsible for stabilizing the iron complexes at neutral pH values.

Therefore, the synthesis of the hexadentate chelator (**catTHC**) consisted on the amide linkage of three units of 2,3-dibenzyloxybenzylamine **2** to the selected tripodal anchor **1** based on a tetrahedral carbon atom (Scheme 1). This hexadentate chelator was designed to be directly compared with the **CP256** analogue having three 3-hydroxy-4-pyridinone units connected to the same backbone [18].

(Please insert Scheme 1)

The amide forming reaction from 2,3-dibenzyloxybenzylamine **2** and the selected tripodal anchor **1** was screened using two coupling reagent pairs: (i) *N*,*N*'-dicyclohexylcarbodiimide (DCC)/*N*-hydroxybenzotriazole (HOBt) and (ii) 1-[3-(dimethyl-amino)propyl]-3-ethylcarbodiimide hydrochloride (EDAC)/*N*-hydroxysuccinimide (NHS). The results obtained are presented in Table 1 and demonstrate that the pair EDAC/NHS gives higher yields (84%) using the room temperature protocol (entry 2), in opposite to the pair DCC/HOBt that only gives 44% of yield (entry 1). Microwave-assisted organic synthesis was employed as an attempt to improve the yield of DCC/HOBt coupling reaction. Thus, using microwave irradiation protocol at 55 ºC, during 15 and 30 min, the yields were 42 and 56%, respectively (entries 3 and 4). These results showed that the microwave irradiation allows to reduce significantly the reaction time from days (3 days) to minutes (15 or 30 min), keeping a similar reaction yield. We have also attempted to carry out the same microwave protocol (55 ºC, 30 min) with the pair EDAC/NHS but, in this case the yield was significantly lower (bellow 30%). According to the results obtained in the amide-forming reaction, the best coupling reagent pairs are EDAC/NHS at room temperature and DCC/HOBt under microwave irradiation.

The subsequent removal of the benzyl protecting groups was carried out with BCl_3 in dichloromethane, under argon atmosphere, affording the final hexadentate chelator (**catTHC**) in 67% of yield.

(Please insert Table 1)

The **catTHC** chelator was characterized by NMR, absorption spectroscopy, mass spectrometry and elemental analysis. The comparison between the ^{1}H NMR spectra of **3** and **catTHC** is presented in Fig. 2 and the most important proton delocalizations are indicated using the symbols ∗, †, ‡, #. The ^{1}H NMR spectrum of the protected ligand **3** (Fig. 2A) displayed a resonance signal at 8.16 ppm due to the $HNCH_2$ protons of the amide linkage. Upon removal of the benzyl protecting groups, this characteristic signal shifted to 8.34-8.40 ppm, which is indicative for intramolecular hydrogen bonding. On the other hand, the ^{1}H NMR spectrum of **catTHC** (Fig. 2B) showed the disappearing of benzyl signals and the appearing of a multiplet at 7.15-7.25 ppm attributed to the resonance of the

OH protons. The chemical shift values found for the proton of the amide links are typical of this amide reversed function -NHCO- and are also similar to those obtained for the tripodal 3-hydroxy-4-pyridinone (**CP256**), where the $HNCH_2$ signal appears at 8.93 ppm [18].

(Please insert Figure 2)

Ligand Acidity Constants and Speciation

In this work, the values of the acidity constants were determined by a spectrophotometric method since the hexadentate ligand was not sufficiently soluble to allow a potentiometric determination [29,30] – the compound precipitation occurs for concentrations above 10^{-4} M. The pK_a values for 2,3-dihydroxybenzaldehyde (commercial compound used as the starting material for 2,3-dibenzyloxybenzylamine **2**) were also determined and the related spectra together with those of its interaction with Fe(III) with pH variation are presented in Supporting Information.

The acidity constants of **catTHC** were determined using equations (1) and (2) (section 2.3) and six values were calculated using the program pHab 2006 [25]. The six pK_a values are listed in Table 2 and two sets of values can be identified, one close to 8 and the second close to 11. These two sets of values are typical pK_a values found for bidentate catechols. The values are in close agreement with those of other catecholate hexadentate chelators prepared with different molecular frameworks [31].

(Please insert Table 2)

The first three acidity constants of **catTHC** (pK_{an}; n = 1-3) are assigned to the more acidic *ortho* OH group on the catechol. The intrinsic acidity of the *ortho* hydroxyl groups are higher relative to the *meta* hydroxyl groups, and this is primarily due to the conjugation of the *ortho* hydroxyl with the amide group [32]. The average pK_a of the first three acidity constants for **catTHC** is 7.57, which is in agreement with the pK_a of the first acidity constant, 7.97, of the bidentate catechol 2,3-dihydroxybenzaldehyde. However, the average of the last three pK_a constants for **catTHC**, 11.1, is smaller than the pK_a of the second acidity constant of 2,3-dihydroxybenzaldehyde (12.22). This difference can be attributed to

the presence of the amide carbonyl function of the backbone, as the amide carbonyl groups are known to lower the protonation constants [23,33,34]. These results are similar to results obtained for enterobactin and MECAM, a synthetic enterobactin analogue [34]. The distribution diagram, obtained with the program Hyss 2006 [23], for compound **catTHC** presented in Fig. 3 reveals that the form $[H_6L]$ predominates at acidic pH, $[H_5L]$ is the major species, with ~65%, between pH 6.5-8, $[H_3L]$ is predominant between pH 8 and 11 and [L] dominates for pH above 11.5. All the other species, namely $[H_4L]$, $[H_2L]$ and [HL] are present in smaller percentages of formation, ~40% at pH ~8 for $[H_4L]$, ~40% at pH ~10.5 for $[H_2L]$ and ~40% at pH ~11.5 for [HL].

(Please insert Figure 3)

Fe(III)-Ligand Complex Stability

As we were interested in verifying the potential application of the **catTHC** hexadentate ligand as an iron(III) chelator we also determine its iron(III)-ligand complex stability and protonation constants using a model of competition with EDTA.

Catechols produce strongly colored iron(III) complexes [35], which exhibit intense ligand-to-metal charge transfer (LMCT) bands. Typically, catechols form three different iron(III) complexes as a function of the pH: (i) at pH< 5 gives rise to the mono(catecholate)iron(III) complex [Fe(cat)]; (ii) at 6< pH< 7 the bis(catecholate)iron(III) complex $[Fe(cat)_2]$ is formed and (iii) at pH> 9.5 the tris(catecholate)iron(III) complex $[Fe(cat)_3]$ is obtained. In general, the stability of the iron(III) – catecholate complexes depends on the catecholate ligand, the extent of the co-ordination to Fe(III) and the pH [36]. High spin iron(III) has an optimum fit for a cation in an octahedral field generated by three catechol functions [6]. Spectrophotometric titration allows us to observe changes in the intense LMCT band of the metal complex as a function of pH, thereby providing a probe to monitor the successive protonation of Fe(III) and **catTHC** complexes [31].

The stability constant of the iron(III) complex with **catTHC** was determined by competition studies against the ligand EDTA using UV-Vis spectroscopy as previously described [37]. An equilibrium time period of 24 h was used since several reports state that

equilibrium between hexadentate ligands and iron(III) are relatively slow and the system needs time to achieve equilibrium [38,39].

The UV-Vis spectra of solutions of the ligand in the presence of iron(III) show a characteristic LMCT band (490 nm) of the iron(III) complex at pH values above 8 (Fig. 4). The red color of the resulting solution is attributed to the LMCT band of the $[FeL]^{3-}$ complex (λ_{max}=490 nm, ε =26261 $M^{-1}cm^{-1}$, pH>9), which is consistent with iron(III) coordination through the six oxygen atoms of the catecholate ligands [35,36,40].

(Please insert Figure 4)

The model used to determine the stability constants was based in Eqs. 1 and 2 (section 2.3.) considering the following equilibriums:

$$[Fe]^{3+}(aq) + [L]^{6-}(aq) \rightleftharpoons [FeL]^{3-}(aq) \qquad (\log \beta_{110})$$

$$[Fe]^{3+}(aq) + [L]^{6-}(aq) + [H]^{+} \rightleftharpoons [FeHL]^{2-}(aq) \qquad (\log \beta_{111})$$

$$[Fe]^{3+}(aq) + [L]^{6-}(aq) + 2\,[H]^{+} \rightleftharpoons [FeH_2L]^{1-}(aq) \qquad (\log \beta_{112})$$

$$[Fe]^{3+}(aq) + [L]^{6-}(aq) + 3\,[H]^{+} \rightleftharpoons [FeH_3L]\ (aq) \qquad (\log \beta_{113})$$

$$[Fe]^{3+}(aq) + [L]^{6-}(aq) + 4\,[H]^{+} \rightleftharpoons [FeH_4L]^{1+}(aq) \qquad (\log \beta_{114})$$

$$[Fe]^{3+}(aq) + [L]^{6-}(aq) + 5\,[H]^{+} \rightleftharpoons [FeH_2L]^{2+}(aq) \qquad (\log \beta_{115})$$

$$[Fe]^{3+}(aq) + [L]^{6-}(aq) + 6\,[H]^{+} \rightleftharpoons [FeH_6L]^{3+}(aq) \qquad (\log \beta_{116})$$

and also the equilibrium constants of $[H_6L]$, EDTA, Fe(III)/EDTA, iron hydroxide species and the autoprotolysis of water.

The results obtained show the predominance of $[FeL]^{3-}$ formation and no additional species could be detected from the data.

The log β_{110} and pFe^{3+} values (calculated as $-\log|Fe^{3+}|$ at pH 7.40 with a total ligand and Fe(III) concentrations of 10^{-5} M and 10^{-6} M, respectively) obtained for **catTHC** were calculated and the values obtained were 36.70±0.03 and 26.7, respectively.

The following distribution diagram considers the percentage of formation of the different species in solution relative to [L] (Fig. 6). The complex $[FeL]^{3-}$ is the major specie for pH above ~7 and $[H_6L]$ for lower pH values.

(Please insert Figure 5)

Conclusions

The values of log β_{110} and pFe^{3+} of **catTHC** are compared with several siderophores in Table 3.

(Please insert Table 3)

The value of the stability constant obtained for the hexadentate catecholate iron(III) complex whose structure is depicted in Fig. 6 is higher than that of the equivalent tripodal 3,4-HPO derivative (**CP256**), as expected for catecholate units since they provide higher stability constants when compared to 3,4-HPO units. However the value found for pFe^{3+} is smaller (26.7 vs 29.84) a trend usually observed for ligands derived from catechol and 3,4-HPO [43,45].

In comparison with enterobactin the new ligand **catTHC** provides lower values of stability constant and pFe^{3+}, a fact that can be explained due to the inexistence of the additional stabilization present in the ferric enterobactin complex associated to the protonated salicylate binding mode [20].

(Please insert Figure 6)

Appendix A. Supplementary data

Supplementary information containing NMR spectra of the protected hexadentate ligand **3** and **catTHC** and UV-Vis spectra of 2,3-dihydroxybenzaldehyde, with or without Fe(III) addition and pH variation are available online, as well as the distribution diagrams as a function of pH and iron(III), including the hydrolytic species.

Acknowledgements

This work received financial support from the European Union (FEDER funds through COMPETE) and National Funds (FCT, Fundação para a Ciência e Tecnologia) through project Pest-C/EQB/LA0006/2013. The work also received financial support from the European Union (FEDER funds) under the framework of QREN through Project NORTE-07-0124-FEDER-000066. The Bruker Avance III 400 MHz NMR spectrometers were purchased under the framework of the National Programme for Scientific Re-equipment, contract REDE/1517/RMN/2005, with funds from POCI 2010 (FEDER) and (FCT) and under the framework of QREN, through project NORTE-07-0162-FEDER-000048. All the spectrometers are part of the National NMR network. To all financing sources the authors are greatly indebted.

References

[1] Crisponi, G.; Remelli, M. *Coord. Chem. Rev.* **2008**, *252*, 1225-1240. doi:10.1016/ j.ccr.2007. 12.014.

[2] Bao, G.; Clifton, M.; Hoette, T. M.; Mori, K.; Deng, S.-X.; Qiu, A.; Viltard, M.; Williams, D.; Paragas, N.; Leete, T.; Kulkarni, R.; Li, X.; Lee, B.; Kalandadze, A.; Ratner, A. J.; Pizarro, J. C.; Schmidt-Ott, K. M.; Landry, D. W.; Raymond, K. N.; Strong, R. K.; Barasch, J. *Nat. Chem. Biol.* **2010**, *6*, 602-609. doi:10.1038/nchembio.402.

[3] d'Hardemare, A.; Torelli, S.; Serratrice, G.; Pierre, J.-L. *Biometals* **2006**, *19*, 349-366. doi: 10. 1007/s10534-005-2997-2.

[4] Hider, R. C.; Kong, X. *Nat. Prod. Rep.* **2010**, *27*, 637-657. doi: 10.1039/b906679a.

[5] Neilands, J. B. *J. Biol. Chem.* **1995**, *270*, 26723-26726. doi 10.1074/jbc.270.45.26723

[6] Tristani, E. M.; Wirgau, J. I.; Dubay, G. R.; Sibert, J. W.; Crumbliss, A. L. *Inorg. Chim. Acta* **2010**, *363*, 3611-3615. doi:10.1016/j.ica.2010.05.052.

[7] Dey, R. K.; Airoldi, C. *J. Hazard. Mat.* **2008,** *156*, 95-101. doi:10.1016/j.jhazmat. 2007.12.005.

[8] Zhou, T.; Ma, Y.; Kong, X.; Hider, R. C. *Dalton Trans.* **2012,** *41*, 6371-6389. doi: 10.1039/ c2dt12159j.

[9] Roosenberg, J. M., 2nd; Lin Ym Fau - Lu, Y.; Lu Y Fau - Miller, M. J.; Miller, M. J. *Curr. Med. Chem.* **2000**, *7*, 159-197. doi: 10.2174/0929867003375353.

[10] Ji, C.; Miller, P. A.; Miller, M. J. *J. Am. Chem. Soc.* **2012**, *134*, 9898-9901. doi: 10.1021/ ja303446w.

[11] Ji, C.; Juárez-Hernández, R. E.; Miller, M. J. *Future Med. Chem.* **2012**, *4*, 297-313. doi:10.4155/fmc.11.191.

[12] Zheng, T.; Bullock, J. L.; Nolan, E. M. *J. Am. Chem. Soc.* **2012**, *134*, 18388-18400. doi: 10. 1021/ja3077268.

[13] Wencewicz, T. A.; Long, T. E.; Möllmann, U.; Miller, M. J. *Bioconj. Chem.* **2013**, *24*, 473-486. doi: 10.1021/bc300610f.

[14] Sahoo, S. K.; Sharma, D.; Bera, R. K.; Crisponi, G.; Callan, J. F. *Chem. Soc. Rev.* **2012**, *41*, 7195-7227. doi: 10.1039/c2cs35152h.

[15] Stintzi, A.; Barnes, C.; Xu, J.; Raymond, K. N. *Proc. Nat. Acad. Sci.* **2000**, *97*, 10691-10696. doi: 10.1073ypnas.200318797.

[16] Loomis, L. D.; Raymond, K. N. *Inorg. Chem.* **1991**, *30*, 906-911. doi: 10.1021/ ic00005a008.

[17] Fernandes, S. S.; Nunes, A.; Gomes, A. R.; de Castro, B.; Hider, R. C.; Rangel, M.; Appelberg, R.; Gomes, M. S. *Microb. Infect.* **2010**, *12*, 287-294. doi:10.1016/j.micinf. 2010.01.003.

[18] Nunes, A.; Podinovskaia, M.; Leite, A.; Gameiro, P.; Zhou, T.; Ma, Y.; Kong, X.; Schaible, U.; Hider, R.; Rangel, M. *J. Biol. Inorg. Chem.* **2010**, *15*, 861-877. doi: 10.1007/s00775-010-0650-1.

[19] Moniz, T.; Nunes, A.; Silva, A. M. G.; Queirós, C.; Ivanova, G.; Gomes, M. S.; Rangel, M. *J. Inorg. Biochem.* **2013,** *121*, 156-166. doi:10.1016/j.jinorgbio.2013.01.002.

[20] Abergel, R. J.; Warner, J. A.; Shuh, D. K.; Raymond, K. N. *J. Am. Chem. Soc.* **2006**, *128*, 8920-8931. doi: 10.1021/ja062046j.

[21] Newkome, G. R.; Behera, R. K.; Moorefield, C. N.; Baker, G. R. *J. Org. Chem.* **1991**, *56*, 7162-7167. doi**:** 10.1021/jo00025a038.

[22] Queirós, C.; Silva, A. M. G.; Lopes, S. C.; Ivanova, G.; Gameiro, P.; Rangel, M. *Dyes Pigm.* **2012**, *93*, 1447-1455. doi:10.1016/j.dyepig.2011.10.010.

[23] Alderighi, L.; Gans, P.; Ienco, A.; Peters, D.; Sabatini, A.; Vacca, A. *Coord. Chem. Rev.* **1999**, *184*, 311-318. doi: 10.1016/S0010-8545(98)00260-4.

[24] Albert, E. P. S. A. *The determination of ionization constants: a laboratory manual*. 2nd ed.; Chapman & Hall: London, 1984.

[25] Gans, P.; Sabatini, A.; Vacca, A. *Ann. Chim.* **1999**, *89*, 45-49.

[26] Martell, A. E.; Smith, R. M. *Critical stability constants*. Plenum Press: New York, 1974; Vol. 1.

[27] Liu, Z. D.; Kayyali, R.; Hider, R. C.; Porter, J. B.; Theobald, A. E. *J. Med. Chem.* **2002**, *45*, 631-639. doi: 10.1021/jm010817i.

[28] Liu, Z. D.; Hider, R. C. *Coord. Chem. Rev.* **2002**, *232*, 151-171. doi: 10.1016/S0010-8545 (02)00050-4.

[29] Öğretir, C.; Demirayak, S. e.; Duran, M. *J. Chem. Eng. Data* **2010**, *55*, 1137-1142. doi: 10. 1021/je9005739.

[30] Guerra, K. P.; Delgado, R. *Dalton Trans.* **2008**, 539-550. doi: 10.1039/b712916e.

[31] Baral, M.; Sahoo, S. K.; Kanungo, B. K. *J. Inorg. Biochem.* **2008**, *102*, 1581-1588. doi:10. 1016/j.jinorgbio.2008.02.006.

[32] Llinas, M.; Wilson, D. M.; Neilands, J. B. *Biochem.* **1973,** *12*, 3836-3843. DOI: 10. 1021/bi00744a007.

[33] Hay, B. P.; Dixon, D. A.; Vargas, R.; Garza, J.; Raymond, K. N. *Inorg. Chem.* **2001**, *40*, 3922-3935. doi: 10.1021/ic001380s.

[34] Dhungana, S.; Heggemann, S.; Heinisch, L.; Möllmann, U.; Boukhalfa, H.; Crumbliss, A. L. *Inorg. Chem.* **2001**, *40*, 7079-7086. doi: 10.1021/ic0104003.

[35] Sever, M. J.; Wilker, J. J. *Dalton Trans.* **2004,** 1061-1072. doi: 10.1039/ b315811j.

[36] Sanchez, P.; Galvez, N.; Colacio, E.; Minones, E.; Dominguez-Vera, J. M. *Dalton Trans.* **2005**, 811-813. doi:10.1039/b416669h.

[37] Dhungana, S.; Ratledge, C.; Crumbliss, A. L. *Inorg. Chem.* **2004**, *43*, 6274-6283. doi: 10.1021/ic049343e.

[38] Harris, W. H.; Raymond, K. N. *J. Am. Chem. Soc.* **1979**, *101*, 6534-6541. doi: 10.1021/ ja00516a010.

[39] Imbert, D.; Thomas, F.; Baret, P.; Serratrice, G.; Gaude, D.; Pierre, J.-L.; Laulhere, J.-P. *New J. Chem.* **2000**, *24*, 281-288. doi: 10.1039/b000229l.

[40] Mies, K. A.; Gebhardt, P.; Möllmann, U.; Crumbliss, A. L. *J. Inorg. Biochem.* **2008**, *102*, 850-861. doi:10.1016/j.jinorgbio.2007.11.021.

[41] Rodgers, S. J.; Lee, C. W.; Ng, C. Y.; Raymond, K. N. *Inorg. Chem.* **1987,** *26*, 1622-1625. doi: 10.1021/ic00257a030.

[42] Sahoo, S. K.; Baral, M.; Kanungo, B. K. *J. Chem. Eng. Data* **2011,** *56*, 2849-2855. doi: 10. 1021/je101338m.

[43] Harrington, J. M.; Chittamuru, S.; Dhungana, S.; Jacobs, H. K.; Gopalan, A. S.; Crumbliss, A. L. *Inorg. Chem.* **2010,** *49*, 8208-8221. doi: 10.1021/ic902595c.

[44] Schwarzenbach, G.; Schwarzenbach, K. *Helv. Chim. Acta* **1963,** *46*, 1390-1400. doi: 10. 1002/hlca.19630460434.

[45] Zhou, T.; Neubert, H.; Liu, D. Y.; Liu, Z. D.; Ma, Y. M.; Kong, X. L.; Luo, W.; Mark, S.; Hider, R. C. *J. Med. Chem.* **2006,** *49*, 4171-4182. doi: 10.1021/jm0600949.

Fig. 1. (A) Structures of enterobactin and **CP256**. (B) Structure of **catTHC**.

Scheme 1. Synthesis of **catTHC**.

Table 1. Yields for the amide-forming reaction of **1** and 2,3-dibenzyloxybenzylamine **2**.

Fig. 2. Partial ^{1}H NMR spectra in DMSO-d^{6} of compounds: (A) **3** and (B) **catTHC**. The symbols ∗, †, ‡, # represent the delocalization of the correspondent protons ($\underline{H}NCH_2$, N$\underline{H}$, H-catechol and $HNC\underline{H_2}$), from compound **3** to **catTHC** in the NMR spectra.

Table 2. pK_a values for 2,3-dihydroxybenzaldehyde and hexadentate catecholate ligand (**catTHC**).

Fig. 3. Distribution diagram as a function of pH of **catTHC**, ~6×10^{-5} M, I = 0.1 M NaCl, 25 ºC.

Fig. 4. UV-Vis spectra of **catTHC**, Fe(III) and EDTA solutions, |**catTHC**| = |Fe^{3+}| ~ 2×10^{-4} M, |EDTA| ~ 1.2×10^{-3} M, I = 0.1 M NaCl, 25 ºC, pH~5.5 to pH~12, after 24 h.

Fig. 5. Distribution diagram as a function of pH of **catTHC**/Fe^{3+}, |**catTHC**| = |Fe^{3+}| ~ 2.0×10^{-4} M, I = 0.1 M NaCl, 25 ºC, 24 h.

Table 3. Values of log β_{110} and pFe^{3+} of siderophores and of hexadentate catecholate ligand (**catTHC**).

Fig. 6. Chemical structure of **FecatTHC** obtained after minimization with ChemDraw 3D.

A

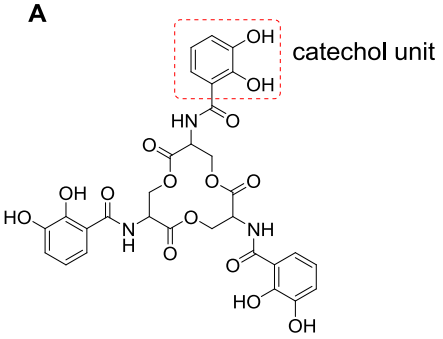

Enterobactin

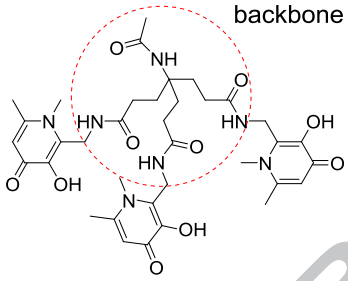

CP256

B

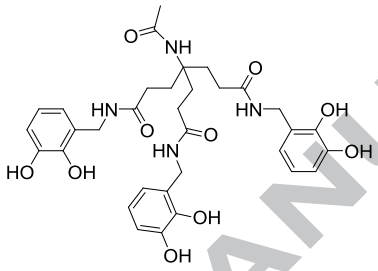

catTHC

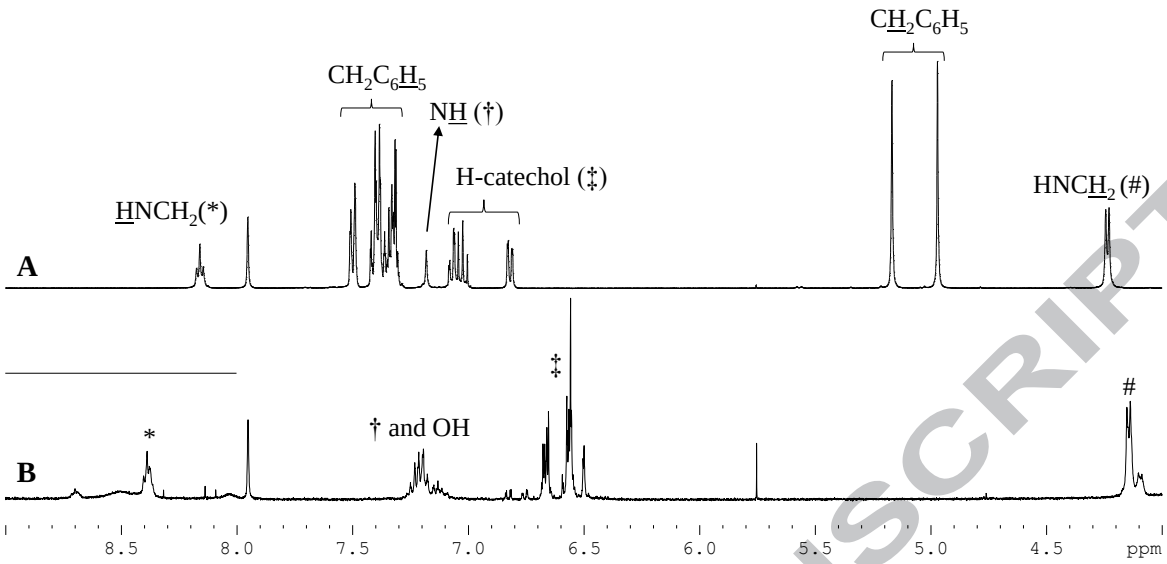

A

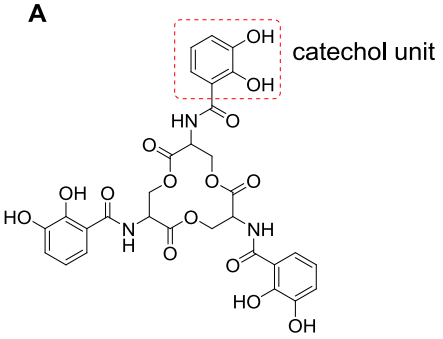

Enterobactin

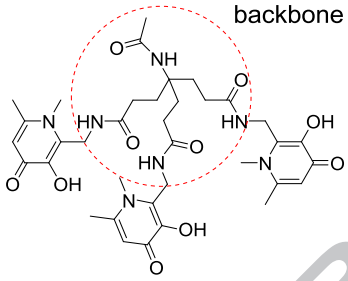

CP256

B

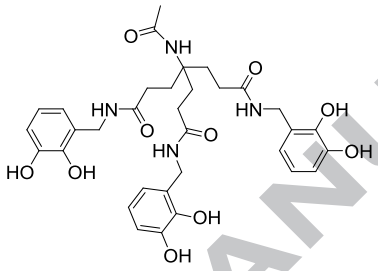

catTHC

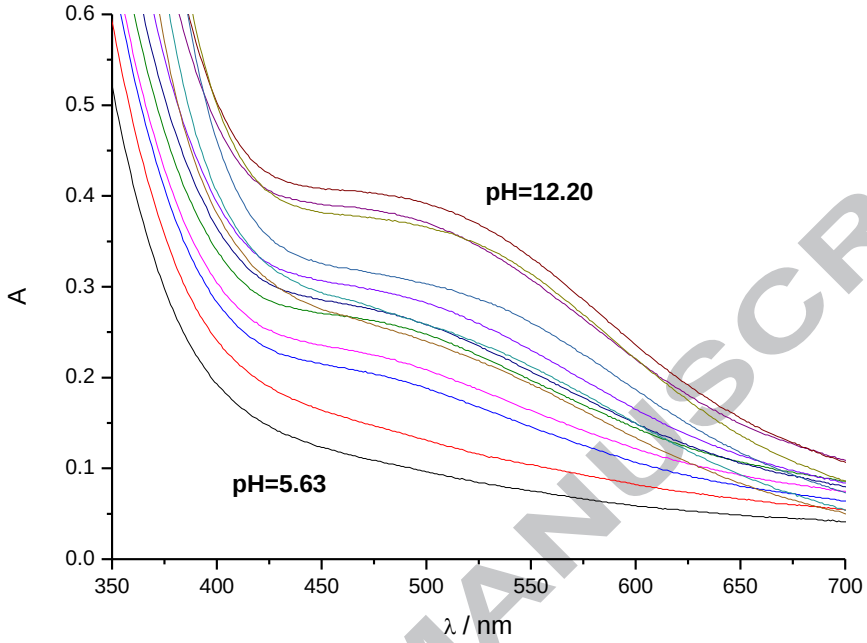

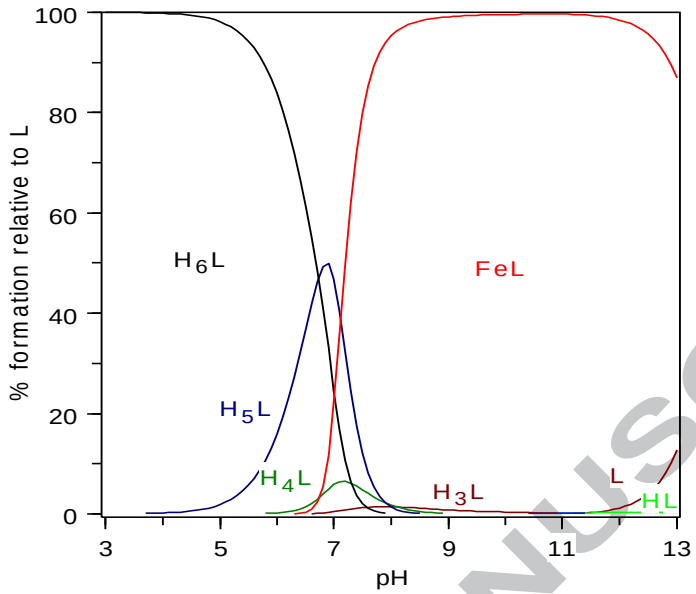

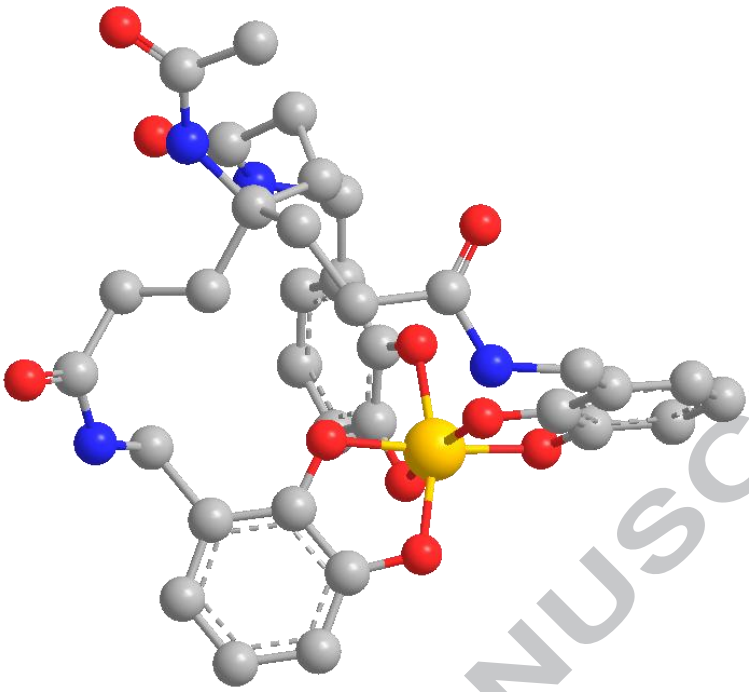

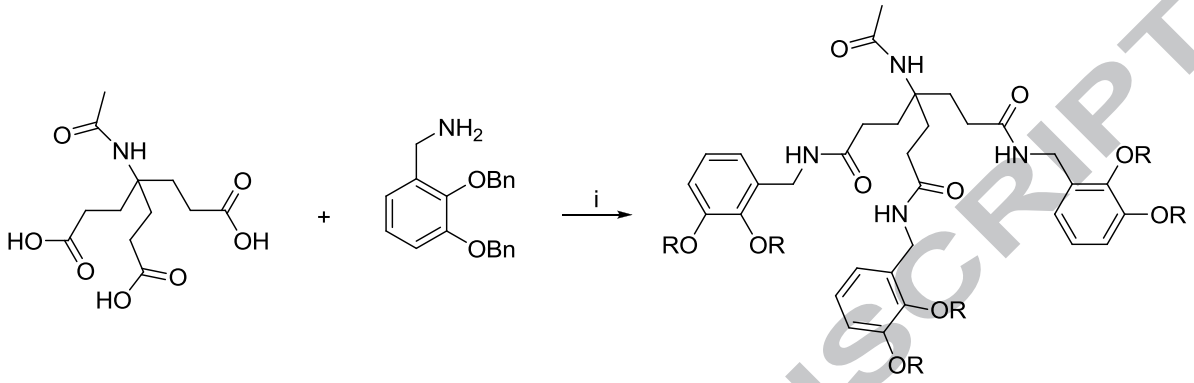

1 **2**

3, R= Bn
catTHC, R= H ii

i. coupling reagents, r.t. or MW
ii. BCl_3, CH_2Cl_2

Entry	Coupling reagent	Temp	Time	Yield (%)
1	DCC/HOBt	r.t.	3 days	44
2	EDAC/NHS	r.t.	2 days	84
3	DCC/HOBt	MW, 55ºC	15 min	42
4	DCC/HOBt	MW, 55ºC	30 min	56

pK_{an}	2,3-dihydroxybenzaldehyde	**catTHC**
n=1	7.97±0.02	6.72±0.09
n=2	12.21±0.06	7.9±0.1
n=3		8.1±0.2
n=4		10.8±0.2
n=5		11.1±0.2
n=6		11.4±0.1

Siderophore	Ligand architecture	log β	pFe^{3+}	Reference
catTHC	Tripodal, catechol	36.70	26.7	This work
CP256	Tripodal, 3,4-HPO	34.40	29.84	[18]
Enterobactin	Tripodal, catechol	49	35.5	[16]
Mycobactin	Linear, bishydroxamate, *N*-(oxazoline) and OH (salycilic acid)	31	29.0	[18]
TREMCAM	Tripodal, catechol	43.2	29.6	[41]
CYCOENCAT	Tripodal, catechol	34.61	24.76	[42]
HOPObactin	Tripodal, 3,4-HPO	26.7	27.4	[43]
Deferoxamine	Linear, trishydroxamate	31.00	26.60	[44]
H_6L[a]	Tripodal, monohydroxa-mate, bis-catecholate	31.4	18.3	[40]
EDTA	Tripodal	25.1	23.4	[4]

[a] N^{α},-N^{β}-Bis[2,3-dihydroxybenzoyl]-*L*-lysyl-(γ-N-methyl-N-hydroxyamido)-L-glutamic acid

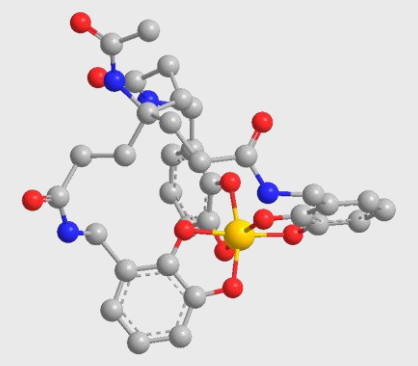

A new tripodal hexadentate chelator (**catTHC**) was synthesized by reaction of a flexible tripodal backbone with three bidentate catechol units. The acid-base properties of the ligand in aqueous solution and the affinity of the ligand towards iron(III) were investigated at variable pH and in the presence of iron(III) using spectroscopic methods. The values obtained for the stability constant and pFe^{3+} are $\log \beta_{110} = 36.70$ and $pFe^{3+} = 26.7$.